

Potential energy curves and dipole transition moments for excited electronic states of XeKr and ArNe

Ioannis D. Petsalakis and Giannoula Theodorakopoulos^{a)}

*Theoretical and Physical Chemistry Institute, The National Hellenic Research Foundation,
48 Vassileos Constantinou Ave., Athens 116 35 Greece*

Heinz-Peter Liebermann and Robert J. Buenker

University of Wuppertal, Fachbereich 9, Theoretische Chemie, Gausstr. 20, D-42097 Wuppertal, Germany

(Received 6 March 2002; accepted 29 May 2002)

Relativistic core-potential calculations have been carried out on Ω states resulting from the interaction of Xe^* ($5p^56s$, 3P , 1P) with ground-state Kr atoms as well as for the system Ar^* ($3p^54s$, 3P , 1P) with ground-state Ne, using different basis sets and configuration interaction procedures. The present calculations on ArNe, employing larger sets of Rydberg functions than those of the previous calculations, yield totally repulsive potentials for the excited states of ArNe. Similar calculations on XeKr obtain shallow minima ($600\text{--}860\text{ cm}^{-1}$) in the potential energy curves of the excited states at large internuclear distances ($6.9\text{--}7.8$ bohr). Dipole transition moments have been calculated and strong radiative transitions are predicted from excited states to the ground state. The $1(I)$ state, correlating with the metastable 3P_2 state of Xe is found to have a small but nonzero dipole transition moment at short and intermediate nuclear distances leading to a radiative lifetime for the $v=0$ level of this state of $21.0\ \mu\text{s}$. © 2002 American Institute of Physics.
[DOI: 10.1063/1.1494796]

I. INTRODUCTION

The excited states of diatomic rare-gas molecules are important for their role as radiation sources in the vacuum ultraviolet (VUV) region, including excimer lasers.^{1–3} While most experimental and theoretical work has been devoted to homonuclear systems, the heteronuclear systems have also attracted interest following the observation of very efficient energy transfer processes in admixtures of rare gases,^{1,4–6} and this opens new possibilities for the efficient pumping of these systems.⁷ The advent of experimental studies of thermal energy collisions between excited and ground-state rare-gas atoms^{8,9} offers a challenge to theoreticians to provide interpretations of the resulting experimental data. Accurate potential energy curves are required for the interacting pairs of atoms over a large range of interatomic distances. However, despite the conceptual simplicity of their electronic structure, accurate determinations of the interaction potentials for the heteronuclear dimers are scarce due to computational difficulties involved. The precise determination of the shallow minima generally found in these systems require large configuration interaction (CI) expansions and adequate basis sets, especially in the Rydberg part. Often, minima which have been proposed in experimental work are not found in the calculations, as for example in the excited states of Kr–Ar,¹⁰ while errors of $\pm 300\text{ cm}^{-1}$ in the calculated potential wells are not unexpected.¹¹ Furthermore, it is essential to include spin–orbit coupling in order to calculate the electronic states correctly. The ground-state potential has different requirements from the excited states in terms of polar-

ization functions and exponents of the diffuse functions. Good potentials for the ground states of the RgRg' systems have been reported and one could focus on the excited-state requirements.^{12,13}

Appropriate *ab initio* methods to calculate potential energy curves for the electronic states of these molecules make use of relativistic core potentials and such calculations have been reported for heteronuclear systems such as KrAr,¹⁰ ArNe,¹⁴ XeHe and XeAr¹¹ and more recently ArHe and HeNe.¹⁵ The calculations on ArHe showed that for such systems it is necessary to employ at least a double-zeta Rydberg basis on the heavier atom in order to calculate the potential energy curves free from spurious “bumps” and minima. The previous work on ArNe by the present authors¹⁴ employed a single Rydberg *s* and a single Rydberg *p* function on Ar with the same exponent, which had been optimized with respect to the atomic Ar excitation energy. While this approach resulted in good agreement at the dissociation limits for the atomic excitation energies and also for transition moments, it was found to lead to erroneous results at short and intermediate internuclear distances for the Ar^*+He system.¹⁵ For this reason, it became necessary to re-calculate the potentials for the Ar^* ($3p^54s$) + Ne interaction in the present work, and to correct the previously reported potentials.

The Xe^* ($5p^56s$) + Kr system, which is the main object of the present work, has been studied by spectroscopic methods,^{1–3,7,16–22} while potential energy curves have been calculated by model Hamiltonian methods.^{23,24} Work based on absorption spectra of Xe-rare gas mixtures showed the existence of a quasi-bound XeKr excimer, near $1469.61\ \text{\AA}$, with a well depth of 120 or 166 cm^{-1} at an internuclear distance of 4.78 or $4.36\ \text{\AA}$, depending on the potential pa-

^{a)}Electronic mail: ithe@eie.gr

parameters adopted⁵ and elsewhere, another estimate³ of the well depths as 153 cm⁻¹ for the excited state near the first resonance line of Xe I and 333 cm⁻¹ for the state near the second resonance line of Xe I (at 1295.59 Å)³. Analysis of laser induced fluorescence (LIF) spectra involving transitions from the ground state to the states 0⁺(³P₁) and 1(³P₁) of Xe*Kr indicated a double well potential for the 0⁺ state (with depths of 624 and 101 cm⁻¹ at *r_e* of 3.09 and 5.1 Å) and a very shallow well for the 1 state (52 cm⁻¹ at 5.24 Å).¹⁹ Emission spectroscopy work of solid Kr bombarded with ³P₂ Xe atoms¹⁶ has reported emission at 7.95 eV corresponding to the XeKr 1(³P₂) exciplex with a binding energy of 138 ± 50 cm⁻¹ at *r_e* = 3.20 ± 0.05 Å. Luminescence studies of the XeKr exciplex in liquid and in solid krypton obtained a lifetime of 52 ± 3 ns in the liquid and 50 ± 3 ns in the solid which were assigned to the 1(³P₂) exciplex.¹⁷ However, it is more likely that the reported data should be assigned to the 0⁺(³P₁) exciplex.²⁵ Model potential calculations predict deeper minima for the exciplex states, ranging from 1000–1200 cm⁻¹ [for the 0⁻(³P₂), 1(³P₂), and 0⁺(³P₁) states] and around 300 cm⁻¹ [for the 2(³P₂) and 1(³P₁) states],^{23–25} while simulations of absorption spectra employing Morse potentials with parameters obtained from the above calculations found 170 cm⁻¹ to be a more suitable value for the well-depth of the 1(³P₁) state.²² Thus it is a rather confusing situation, considering that the emission spectra of XeKr overlap with those of the homonuclear dimer, Xe₂ and the fact that the excited states corresponding to a particular limit are closely lying and also lead to overlapping emission spectra.^{1,21,22} Similarly for the next higher states, correlating with excited Xe+ground-state Kr limits, besides the estimated well depth of 333 cm⁻¹ mentioned above,³ Tsuchizawa *et al.*¹⁸ have reported minima of 1445 and 54 cm⁻¹ for the 1(¹P₁) and the 0⁺(¹P₁) states, respectively, while Mao *et al.*²⁰ propose the opposite assignments. Thus despite the aforementioned computational problems, a very careful theoretical study on these systems could shed some light on these issues.

In the present work, multireference configuration interaction calculations (MRDCI) employing relativistic effective core potentials (RECP) have been carried out on Ω states resulting from the interaction of Xe* (5*p*⁵6*s*, ³P, ¹P) with ground-state Kr atoms as well as for the system Ar* (3*p*⁵4*s*, ³P, ¹P) with ground-state Ne, using a variety of basis sets and configuration interaction procedures. Potential energy curves and dipole transition moments have been calculated and radiative lifetimes of the excited states have been determined.

II. CALCULATIONS

The present calculations on XeKr include the ground and excited electronic states correlating with the limits Xe (5*p*⁵6*s*, ³P, ¹P) plus ground-state Kr, and similarly those on ArNe include the ground and excited states correlating with Ar (3*p*⁵4*s*, ³P, ¹P) plus ground-state Ne. In C_{2v} symmetry, the resulting states in each case comprise two ¹A₁ states and one of ³A₁, ¹B₁ and ¹B₂, ³B₁, and ³B₂ symmetry, which correspond to the lowest two ¹Σ⁺, and the lowest ³Σ⁺, ¹Π, and ³Π states, respectively. These states give rise

to Ω states of 0⁺(3), 0⁻(2), 2(1), 1(3) symmetry in the full linear double group and of total C_{2v} symmetry A₁, A₂, B₁, and B₂.^{10,14,15}

The calculations have been carried out with the aid of a relativistic effective core potentials (RECP) version of the MRDCI programs, using the contracted CI implementation^{26–30} which involves a two-step procedure. In the first step Λ-S electronic states are determined in conventional CI calculations in which all the electronic integrals are calculated with the aid of RECPs, whereby the self-consistent field-molecular orbital (SCF-MO) basis is computed in a treatment which includes only the scalar relativistic terms in addition to the conventional nonrelativistic Hamiltonian. The resulting Λ-S states are employed in the second step to form the full Hamiltonian matrix including the spin-orbit interaction. Diagonalization is then carried out for each total symmetry to determine eigenvalues and eigenfunctions. In the present work, the latter are in turn employed for the computation of dipole transition moments between electronic states. These calculations are carried out for different values of the internuclear distance *R*, varying from 4.0 to 20.0 bohr for XeKr and from 3.5 to 20.0 bohr for ArNe and also for *R* = 100 bohr.

Relativistic core potentials are employed for both Xe (K, L, M, and N shells)³¹ and Kr (K, L, and M shells).³² For each atom the Gaussian basis sets for the valence shell^{31,32} were augmented with two sets of *d* and one set of *f* polarization functions with exponents 0.31, 0.15, and 0.5, respectively, for Xe and 0.5, 0.3, and 0.12, respectively, for Kr. The necessary diffuse functions were also included, three *s* (exponents 0.09, 0.055, 0.021), three *p* (exponents 0.07, 0.036, 0.013), and one *d* (exponent 0.058) in the Xe basis set and two *s* (exponents 0.1, 0.05) and two *p* (exponents 0.07, 0.04) in the Kr basis set. Several sets of calculations were carried out employing different diffuse and/or polarization functions and CI procedures in order to establish convergence of the calculated potentials, at least in the qualitative features. The above basis set, with the valence Gaussian functions included in uncontracted form, has been employed to obtain the results that will be discussed in the present work.

In multireference calculations, the choice of reference space is very important because it determines the zeroth-order description of the states, and the CI spaces are generated by allowing single and double excitations with respect to all the reference configurations. The reference spaces employed in the present work, consisting of nine configurations for the ¹A₁ and eight configurations for each of the ³A₁, ¹B₁, ³B₁, ¹B₂ and ³B₂ calculations, have been determined by test calculations at different values of the internuclear distance in each case and they characterize the calculated wave functions throughout with a contribution of over 90%. Exploratory calculations in the present work indicate that it is desirable to have *T*=0 calculations for the potentials, as was also found in our previous work on ArHe and HeNe.¹⁵ For this reason and in order to keep the calculations tractable, the highest energy 14 *a*₁, 8 *b*₁, 8 *b*₂ and 3 *a*₂ virtual orbitals were not included in the CI. This left 22 *a*₁, 12 *b*₁, 12 *b*₂ and 4 *a*₂ MO for the 16-electron CI calculations. The CI spaces include all the configuration functions resulting

TABLE I. Energy levels of Xe($5p^6\ ^1S, 5p^56s\ ^{1,3}P$) + Kr ($2p^6\ ^1S$) and Ar ($3p^6\ ^1S, 3p^54s\ ^{1,3}P$) + Ne ($2p^6\ ^1S$) at 100.0 bohr.

Ω states	XeKr		ArNe	
	ΔE^a present work cm ⁻¹	ΔE experimental cm ⁻¹	ΔE^b present work cm ⁻¹	ΔE experimental ^c cm ⁻¹
0 ⁺ (I)	0.0	0.0 ($J=0$)	0.0	0.0 ($J=0$)
0 ⁻ (I)	67 065		93 138	
1(I)	67 065		93 139	
2(I)	67 068	67 068 ($J=2$)	93 144	93 143.8 ($J=2$)
0 ⁺ (II)	68 126		93 750	
1(II)	68 249	68 046 ($J=1$)	93 779	93 750.6 ($J=1$)
0 ⁻ (II)	76 474	76 197 ($J=0$)	94 553	94 553.7 ($J=0$)
0 ⁺ (III)	77 119		95 389	
1(III)	77 023	77 186 ($J=1$)	95 369	95 399.9 ($J=1$)

^aExcited states shifted by 1731 cm⁻¹.^bExcited states shifted by 3409 cm⁻¹.^cReference 37.

from all single and double excitations with respect to the reference configurations. The resulting CI spaces consist of 211 553 configuration functions (S^2 eigenfunctions) for the 1A_1 , 346 984 for the 3A_1 , 205 712 for the 1B_1 and the 1B_2 and 350 480 configuration functions for the 3B_1 and the 3B_2 calculations. A full-CI correction³³ was applied to the eigenvalues.

The present calculations on ArNe also employed relativistic core potentials for Ar (K and L shells) and Ne (K shell).³⁴ The atomic orbital (AO) basis set employed for Ar is the ($12s9p/6s5p$) basis of McLean and Chandler,³⁵ augmented with one set of d functions for polarization (exponent 0.736) and three s and one p diffuse functions with exponents 0.08, 0.04 and 0.015 and 0.0405, respectively. It was found necessary to employ such a triple-zeta basis for the $4s$ function of Ar in order to obtain convergence in the resulting potentials. For Ne the ($11s6p/5s4p$) basis of Dunning³⁶ was augmented with one polarization d (exponent 0.8) and one s and one p diffuse (exponents 0.03 and 0.025, respectively) functions. As in the above calculations, the CI strategy was to carry out $T=0$ calculations, to insure as uniform a description over the different internuclear distances as possible. To achieve this, the highest 8 a_1 , 3 b_1 , and 3 b_2 virtual MO were removed. Again 16-electron CI calculations were carried out employing reference spaces of eight configurations for the 1A_1 and seven configurations for each of the 3A_1 , 1B_1 , 3B_1 , 1B_2 , and 3B_2 calculations. The CI spaces included 177 880 configuration functions for the 1A_1 calculation, 174 110 for the 1B_1 and 1B_2 , 288 896 for the 3A_1 and 296 233 configuration functions for the 3B_1 and 3B_2 calculations.

The computed excitation energies at the internuclear distance of 100.0 bohr for both XeKr and ArNe are listed in Table I, along with the experimental values³⁷ for the levels of Ar* and Ne*, respectively. The theoretical levels have been shifted upward by 1731 cm⁻¹ for XeKr and by 3409 cm⁻¹ for ArNe, as the calculations tend to favor the Rydberg states over the ground state, for which there is more correlation energy to be accounted for. This is a typical practice in such calculations.^{10,15} As shown in Table I, the calculated splittings of the Xe*($5p^56s, ^3P, ^1P$) and the

Ar*($3p^54s, ^3P, ^1P$) levels are in excellent agreement with the corresponding experimental values.

III. RESULTS AND DISCUSSION

A. Results of calculations on XeKr

In Table II the energies of the Ω excited states of XeKr calculated in the present work are given in cm⁻¹ and with respect to the minimum energy of the ground state. These energies are as obtained after the final diagonalization including the spin-orbit coupling and do not include the shift by 1731 cm⁻¹ mentioned above. The Λ -S potentials are given in Fig. 1 while the corresponding Ω potentials are given in Fig. 2 and finer details for some of these states are given in Figs. 3 and 4. As shown in Fig. 1, the $1^3\Sigma^+$ and the $2^1\Sigma^+ 5p\sigma \rightarrow 6s$ states have Rydberg minima for $R = 5.8$ bohr, close to the minimum of the ground state of the cation XeKr⁺,³⁸ while the $1^3\Pi$ and the $1^1\Pi$ states show rather shallow and wide minima at larger R , close to 8.0 bohr. The corresponding Ω potentials, shown in Fig. 2 along with the Λ -S potentials for comparison, have notably shallower minima occurring at larger R than the potentials of the Λ -S states. As shown in Fig. 2, the spin-orbit coupling has a profound effect on the relative positions of the electronic states. In Fig. 3, enlarged plots of the 0⁻(I), 1(I), 2(I), 1(II), and 0⁺(II) potentials in the region around the energy minima are given. The present results are in qualitative agreement with the previous model potential calculations²³⁻²⁵ (cf. plots of potentials in Krylov *et al.*) although the well depths and the position of the minima are not identical, as will be discussed below. Enlarged plots of the 0⁻(II), 1(III), and 0⁺(III) potentials in the region around the energy minima are given in Fig. 4, while in Fig. 5 the calculated dipole transition moments for the allowed transitions from the excited states to the ground state in XeKr are given.

In Table III, some data relevant to the minima of the excited state potentials of XeKr are given along with the calculated radiative lifetimes for the $v=0, 1, 2$, and 10 levels of the excited states. The calculated potentials have minima ranging between 598 and 860 cm⁻¹, with r_e ranging between 6.9 and 7.8 bohr. Experimental well depths are generally

TABLE II. Calculated total energies^a (cm⁻¹) of excited states of XeKr with respect to the minimum energy of the ground state.

<i>R</i> (bohr)	0 ⁺ (II)	0 ⁺ (III)	2(I)	0 ⁻ (I)	0 ⁻ (II)	1(I)	1(II)	1(III)
4.0	105 486	141 282	135 192	104 610	141 276	104 616	135 809	141 912
4.25	89 715	119 606	113 389	88 971	119 600	88 982	114 051	120 283
4.5	79 818	104 555	98 187	79 144	104 548	79 162	98 874	105 246
4.75	73 793	94 195	87 638	73 144	94 187	73 172	88 358	94 908
5.0	70 280	87 152	80 365	69 627	87 139	69 670	81 120	87 883
5.25	68 335	82 451	75 382	67 665	82 428	67 728	76 170	83 182
5.5	67 331	79 402	71 992	66 631	79 360	66 718	72 815	80 108
5.75	66 841	77 514	69 710	66 111	77 435	66 223	70 570	78 161
6.0	66 607	76 417	68 191	65 857	76 284	65 986	69 094	76 978
6.25	66 503	75 828	67 192	65 731	75 629	65 862	68 146	76 289
6.5	66 453	75 545	66 540	65 667	75 275	65 782	67 557	75 907
6.75	66 441	75 431	66 124	65 634	75 094	65 718	67 203	75 703
7.0	66 440	75 397	65 860	65 614	75 003	65 665	66 997	75 596
7.25	66 459	75 409	65 701	65 604	74 961	65 626	66 881	75 544
7.5	66 481	75 439	65 610	65 604	74 949	65 605	66 822	75 526
7.75	66 523	75 485	65 575	65 616	74 959	65 606	66 802	75 531
8.0	66 570	75 541	65 569	65 638	74 987	65 620	66 808	75 555
8.25	66 620	75 596	65 589	65 670	75 021	65 648	66 831	75 588
8.5	66 678	75 657	65 625	65 706	75 064	65 685	66 866	75 629
8.75	66 732	75 714	65 667	65 743	75 105	65 723	66 903	75 669
9.0	66 782	75 763	65 714	65 778	75 144	65 761	66 941	75 709
9.5	66 865	75 850	65 792	65 837	75 216	65 825	67 007	75 777
10.0	66 916	75 903	65 846	65 876	75 261	65 868	67 050	75 821
10.5	66 958	75 946	65 891	65 909	75 300	65 904	67 086	75 857
11.0	66 995	75 985	65 932	65 942	75 337	65 939	67 121	75 892
11.5	67 032	76 022	65 972	65 976	75 373	65 975	67 156	75 928
12.0	67 064	76 055	66 007	66 008	75 406	66 008	67 189	75 960
12.5	67 092	76 084	66 037	66 036	75 435	66 036	67 217	75 989
13.0	67 115	76 107	66 060	66 057	75 458	66 058	67 239	76 011
14.0	67 155	76 146	66 100	66 095	75 497	66 096	67 278	76 050
15.0	67 186	76 177	66 132	66 126	75 530	66 127	67 309	76 082
16.0	67 209	76 201	66 155	66 148	75 554	66 150	67 333	76 106
17.0	67 223	76 217	66 169	66 163	75 570	66 165	67 347	76 120
18.0	67 232	76 225	66 179	66 174	75 577	66 175	67 357	76 129
19.0	67 240	76 233	66 186	66 182	75 584	66 183	67 364	76 136
20.0	67 245	76 238	66 191	66 187	75 589	66 188	67 369	76 141
100.0	67 264	76 257	66 206	66 203	75 612	66 203	67 387	76 161

^aUnshifted energies.

smaller than the theoretical values, with a variation in the proposed r_e as well, as mentioned above in the Introduction. For the 1(I) state [also denoted 1(³P₂)] the well-depth value of 138 ± 50 cm⁻¹ at an r_0 value of 6.05–6.24 bohr has been

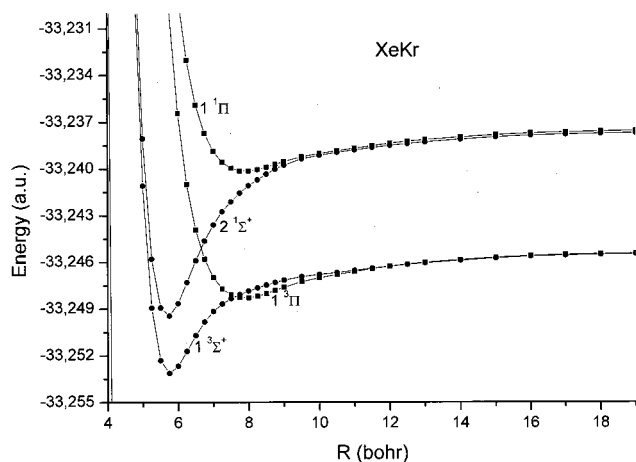


FIG. 1. Potential energy curves for the A-S states of XeKr.

proposed¹⁶ for XeKr in the solid phase, corresponding to emission at 7.95 eV, while other observations of the 1(I) \rightarrow X 0⁺(I) transition also place it at 153–156 nm²² (i.e., a transition energy of 8.1–7.95 eV). The present calculations obtain a higher value for the vertical transition energy of this state (8.3 eV) at the calculated minimum ($R=7.6$ bohr). The dipole transition moment for the 1(I) \rightarrow X 0⁺(I) (cf. Fig. 5) shows a maximum at 6.0 bohr and lower values in the region of the minimum. As a result the computed radiative lifetime for this state is 21.0 μ s for $v=0$, decreasing to 0.6 μ s for $v=10$ (cf. Table III). Thus the present calculations are not in agreement with the results of previous model calculations of the radiative lifetimes²⁵ in which the experimental potential was used for the region near the minimum and according to which the lifetime of the 1(I) state is under 100 ns and increases with vibrational quantum number. However, a plot of the transition probability obtained using the 1(I) \rightarrow X 0⁺(I) dipole transition moments of the present work (Fig. 5), as given in Fig. 6, is very similar to the plot of the radiation width in the previous model calculations,²⁵ showing a steep maximum at 6.0 bohr, at which internuclear distance the transition energy is 8.04 eV, well within the range of ob-

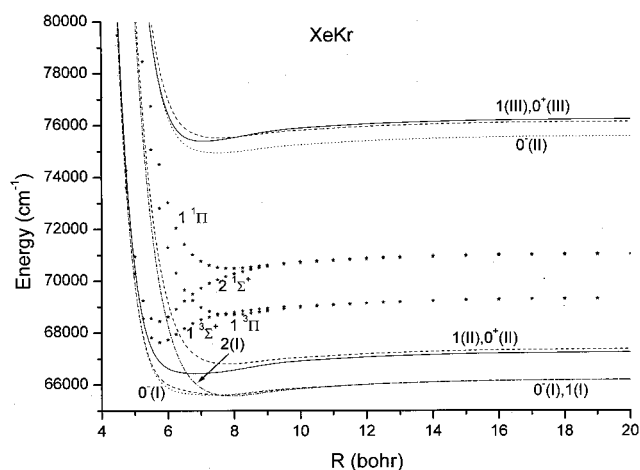


FIG. 2. Potential energy curves for Ω states of Xe^* ($5p^5 6s \ 1,3P$) + $\text{Kr}(2p^6 \ 1S)$.

served values. In view of the difficulties in determining a precise value for the r_e of this state and with only a single experimental deduction, it is difficult to draw further conclusions.

Most of the available spectroscopic work involves the excited states observed near the first resonance line of Xe^* , i.e., $0^+(II)$ and $1(II)$. Generally shallow wells are proposed: Depending on the potential parameters employed² well depths of 120 cm^{-1} at 9.03 bohr or 160 cm^{-1} at 8.2 bohr are estimated on the basis of the absorption spectra.² Another estimate of the minimal dissociation energy for these states is 153 cm^{-1} at a transition energy of 67892 cm^{-1} .³ For the $1(II)$ state Pibel *et al.*¹⁹ propose a well depth of 52.2 cm^{-1} at 5.24 Å (9.90 bohr), while for the $0^+(II)$ state they propose a double well potential with an inner minimum of 624 cm^{-1} at 3.09 Å (5.8 bohr) and an outer minimum of 101 cm^{-1} at 9.6 bohr.¹⁹ Model Hamiltonian calculations obtained 440 cm^{-1} at $r_e = 8.20$ bohr for $1(II)$ and a single minimum of 920 cm^{-1} at $r_e = 6.71$ bohr for $0^+(II)$.^{23,24} Similarly, in the present work, there is no evidence for a double well potential for $0^+(II)$, with a single minimum of 585 cm^{-1} found for this

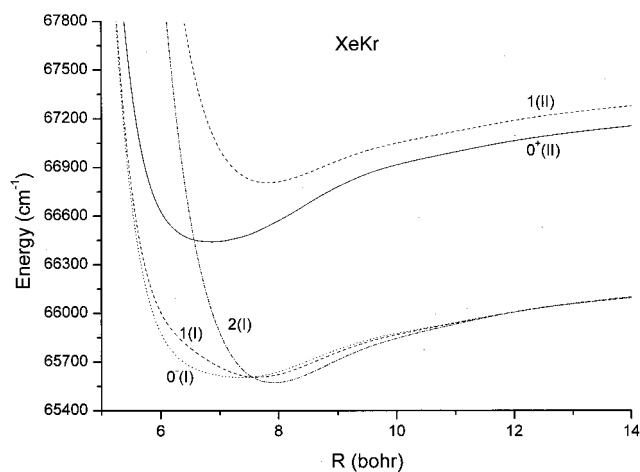


FIG. 3. Potential energy curves of the $0^-(I)$, $1(I)$, $2(I)$, $1(II)$, and $0^+(II)$ states of Xe^*Kr .

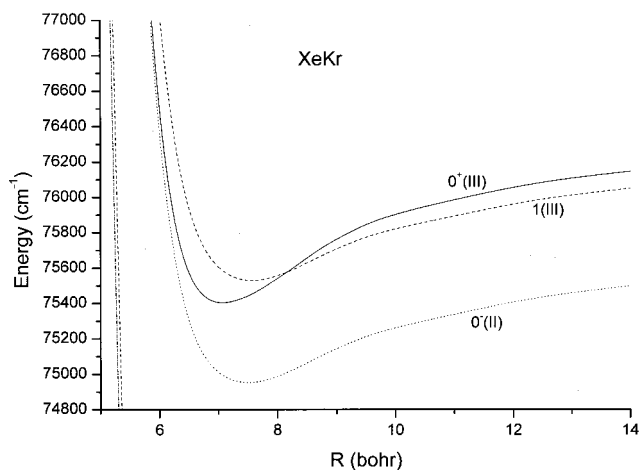


FIG. 4. Potential energy curves of the $0^-(II)$, $1(III)$, and $0^+(III)$ states of Xe^*Kr .

state at 6.9 bohr. It is possible that the experimental deductions¹⁹ might change if the potentials and transition moments of the present work are employed in the analysis of the spectra. Finally, recent experimental work involving emission near 147 nm report that it is not possible to distinguish between emission from $1(II)$ and from the $0^+(II)$ states.^{1,22} These authors favor a well depth of 170 cm^{-1} at 8.3 bohr for $1(II)$. The calculated r_e , ΔE_V and D_e of the present work for these states (cf. Table III) are in reasonably good agreement with experiment.

For the higher states of XeKr computed in the present work, $0^-(II)$, $1(III)$, and $0^+(III)$ there are no previous theoretical calculations. A bound excited state near the second resonance line of Xe^* with well depth of 333 cm^{-1} at a transition energy of 77185.1 cm^{-1} has been proposed in an early absorption spectroscopy study.³ More recent experimental estimates¹⁸ of the interatomic potentials of the $1(III)$ and $0^+(III)$ states yield a dissociation energy of 1445 cm^{-1} for the $1(III)$ state at 5.7 bohr and 54 cm^{-1} for the $0^+(III)$ state at 6.9 bohr, for transition energies 75899.5 and 77293.0 cm^{-1} , respectively. Subsequent work²⁰ reversed the

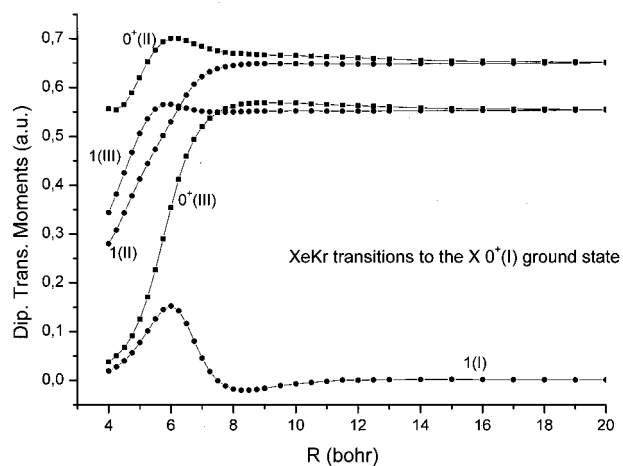


FIG. 5. Calculated transition moments between the excited and the ground state of XeKr .

TABLE III. Calculated molecular constants of excited states of XeKr.

State	r_e bohr	B_e cm^{-1}	ω_e cm^{-1}	ΔE_v^a cm^{-1}	D_e cm^{-1}	$E_{v=0}^b$ cm^{-1}	τ_{rad} ($v=0,1,2,10$)
$0^-(\text{I})$	7.38	0.022	40.27	67 288	599	67 344	...
$1(\text{I})$	7.60	0.021	40.63	67 326	598	67 347	21.0 μs , 6.2 μs , 2.9 μs , 0.6 μs
$2(\text{I})$	7.94	0.019	35.21	67 300	637	67 315	...
$0^+(\text{II})$	6.91	0.025	45.73	67 822	824	68 182	3.4 ns, 3.7 ns, 4.3 ns, 3.5 ns
$1(\text{II})$	7.80	0.019	31.81	68 528	585	68 547	12.5 ns, 4.9 ns, 3.9 ns, 3.7 ns
$0^-(\text{II})$	7.51	0.021	15.27	76 678	663	76 694	...
$0^+(\text{III})$	7.03	0.024	22.98	76 888	860	77 147	4.2 ns, 5.0 ns, 5.7 ns, 3.7 ns
$1(\text{III})$	7.67	0.021	33.14	77 253	635	77 271	10.4 ns, 4.8 ns, 3.8 ns, 3.5 ns

^aWith respect to the ground-state energy at r_e of the excited state, including the shift of 1731 cm^{-1} .

^bWith respect to the ground-state minimum energy, including the shift of 1731 cm^{-1} .

above assignment, proposing that the lower energy transition (to the state with the deeper minimum) is the $0^+(\text{III})-X 0^+(\text{I})$. The transition energies of the present work, $76\,888$ and $77\,253 \text{ cm}^{-1}$ for the $0^+(\text{III})$ and $1(\text{III})$, respectively (cf. Table III), do show that the potential energy curve of the $0^+(\text{III})$ state near the minimum lies below that of the $1(\text{III})$ state (cf. also Fig. 4), and are in good agreement with the observed transition energies. Furthermore, the deepest minima calculated are those of the $0^+(\text{III})$ and $0^+(\text{II})$ states (cf. Table III). There is difficulty in comparing the calculated r_e values for $1(\text{III})$ and $0^+(\text{III})$ with the experimental.^{18,20} It might be noted that the location of the proposed deep minimum at relatively short bond length for the $0^+(\text{III})$ state,²⁰ and also similarly for the $0^+(\text{II})$ state,¹⁹ is close to the position of the minimum in the potential of the $2^1\Sigma^+$ state (cf. Fig. 1), which along with $1^3\Pi$ (mostly) and $X^1\Sigma^+$ interact via spin-orbit coupling to produce the 0^+ states. Similarly, the available experimental r_e estimate for the $1(\text{I})$ state¹⁶ is closer to that of the minimum in the $1^3\Sigma^+$ state (cf. Fig. 1) than to the value calculated for $1(\text{I})$ (cf. Table III).

As might be expected, large dipole transition moments (cf. Fig. 5) and correspondingly short lifetimes (a few nano-

seconds) are obtained for the $0^+(\text{II})$, $1(\text{II})$, $0^+(\text{III})$, and $1(\text{III})$ states (cf. Table III) that correlate with atomic limits which have dipole-allowed transitions to the ground state.

B. Potential energy curves of ArNe

As mentioned in the Introduction, a previous study has been devoted to the potential energy curves of the Ω states of $\text{Ar}(3p^6^1S, 3p^54s^1, ^3P) + \text{Ne}(2p^6^1S)$ in which only a single s and a single set of p diffuse functions optimized at the dissociation limits with respect to the atomic excitation energies were employed.¹⁴ Those calculations obtained both good excitation energies, without the necessity of any shift, and transition moments at the dissociation limits, a reasonably accurate ground-state potential and well depths of about 800 cm^{-1} at internuclear distances of $7.5\text{--}8.5$ bohr for the excited state potentials. However, a subsequent theoretical study of ArHe and HeNe ¹⁵ has shown that the results obtained with the treatment adopted in the work on ArNe ¹⁴ were not stable with respect to changes in the Rydberg basis set and that it is necessary to have a triple-zeta diffuse basis in order to obtain converged results.

The results of the present calculations on the Ω states of ArNe are listed in Table IV, while the potential energy curves are shown in Fig. 7 and the transition moments to the ground state in Fig. 8. As shown in Fig. 7, the potential energy curves for both the Λ -S and the Ω excited states are calculated to be totally repulsive. While the existence of very shallow minima ($\sim 100 \text{ cm}^{-1}$) cannot be excluded, the present calculations do not support the existence of any minima of 800 cm^{-1} depth indicated in the previous study. This result underscores the importance of employing a flexible basis for the Rydberg orbitals in such calculations. More generally, the lack of any experimental information on the excited states of ArNe makes it quite difficult to describe these systems on a definitive basis.

IV. CONCLUSIONS

Relativistic core-potential calculations have been carried out on Ω states resulting from the interaction of Xe^*

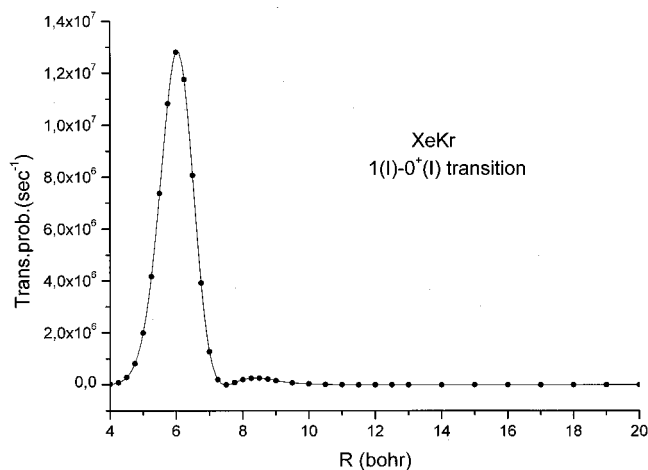


FIG. 6. Calculated radiative transition probability for the $1(\text{I}) \rightarrow X 0^+(\text{I})$ transition.

TABLE IV. Calculated total energies^a (cm⁻¹) of excited states of ArNe with respect to the minimum energy of the ground state.

<i>R</i> (bohr)	0 ⁺ (II)	0 ⁺ (III)	2(I)	0 ⁻ (I)	0 ⁻ (II)	1(I)	1(II)	1(III)
3.50	101 000	112 930	111 928	100 136	112 928	100 138	112 277	113 882
3.75	97 058	104 731	103 709	96 108	104 727	96 113	104 070	105 733
4.00	95 145	99 817	98 762	94 115	99 803	94 125	99 134	100 838
4.25	94 161	96 863	95 733	93 089	96 816	93 109	96 121	97 854
4.75	92 888	94 230	92 676	91 980	93 908	92 025	93 137	94 877
5.00	92 563	93 921	92 162	91 737	93 448	91 782	92 662	94 387
5.25	92 292	93 717	91 801	91 539	93 133	91 577	92 342	94 052
5.50	92 079	93 569	91 540	91 375	92 905	91 404	92 115	93 812
5.75	91 902	93 448	91 331	91 231	92 723	91 251	91 936	93 622
6.00	91 745	93 338	91 154	91 097	92 564	91 110	91 782	93 456
6.25	91 606	93 241	90 999	90 977	92 427	90 982	91 648	93 311
6.50	91 472	93 143	90 852	90 858	92 294	90 856	91 519	93 171
6.75	91 353	93 052	90 725	90 749	92 177	90 743	91 404	93 047
7.00	91 257	92 977	90 623	90 659	92 081	90 649	91 311	92 947
7.25	91 181	92 911	90 544	90 581	92 003	90 571	91 233	92 869
7.50	91 125	92 861	90 486	90 519	91 943	90 510	91 172	92 810
7.75	91 097	92 828	90 459	90 487	91 914	90 480	91 141	92 779
8.00	91 080	92 806	90 444	90 465	91 895	90 460	91 121	92 760
8.25	91 065	92 787	90 431	90 447	91 879	90 443	91 104	92 743
8.50	91 056	92 773	90 423	90 436	91 869	90 432	91 093	92 732
8.75	91 048	92 763	90 415	90 427	91 861	90 424	91 084	92 723
9.00	91 041	92 753	90 409	90 420	91 854	90 417	91 077	92 715
9.50	91 023	92 733	90 391	90 405	91 839	90 401	91 062	92 699
10.0	91 001	92 712	90 370	90 389	91 820	90 384	91 044	92 681
11.0	90 982	92 689	90 352	90 356	91 795	90 355	91 017	92 661
12.0	91 000	92 702	90 372	90 367	91 810	90 369	91 030	92 673
13.0	91 005	92 710	90 375	90 373	91 815	90 375	91 036	92 677
14.0	91 010	92 714	90 381	90 380	91 821	90 380	91 042	92 683
15.0	91 014	92 715	90 386	90 384	91 825	90 384	91 046	92 687
16.0	91 017	92 716	90 389	90 384	91 827	90 385	91 047	92 691
18.0	91 017	92 715	90 390	90 383	91 826	90 385	91 047	92 693
20.0	91 024	92 721	90 397	90 389	91 833	90 391	91 054	92 701

^aUnshifted energies.

($5p^5 6s, ^3P, ^1P$) with ground state Kr atoms as well as for the system Ar* ($3p^5 4s, ^3P, ^1P$) with ground state Ne, using different basis sets and configuration interaction procedures. The present calculations on XeKr obtain shallow minima for the excited states of this system, in generally good qualitative agreement with previous model Hamiltonian calculations. However, the results differ in details such as the depth of the minima, the r_e values and the radiative lifetime of the

1(I) state. It is rather difficult to make quantitative interpretations for the available experimental data on the Ω states of XeKr calculated in the present work because there are considerable variations with regard to the location of the minima among different experimental studies.

The present calculations on ArNe obtain totally repulsive potential energy curves, showing that our previously reported potentials for this system are erroneous. This result indicates that great care is required in calculations of these systems,

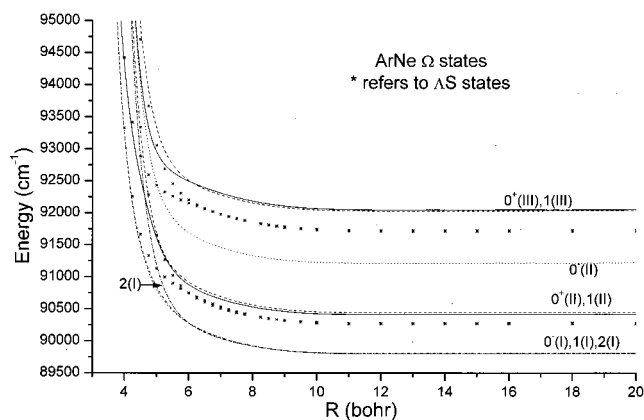
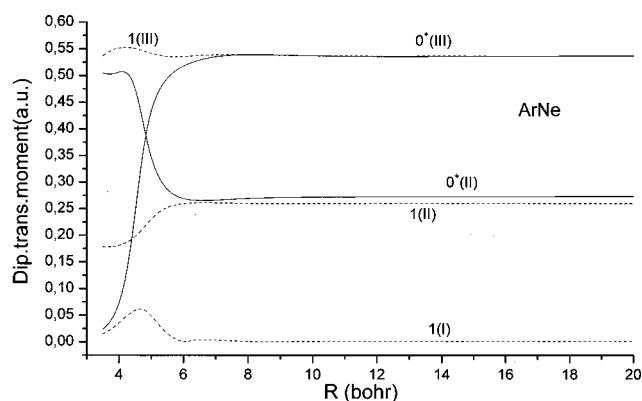
FIG. 7. Potential energy curves for Ω states of Ar* ($3p^5 4s, ^1,3P$) + Ne($2p^6 ^1S$).

FIG. 8. Calculated transition moments between the excited and the ground state of ArNe.

particularly in the choice of the diffuse basis functions employed to describe their Rydberg states.

ACKNOWLEDGMENTS

The present work was supported by NATO CLG 977379 and INTAS OPEN99-0039 as well as from the Verein der Chemischen Industrie.

- ¹B. Krylov, G. Gerasimov, A. Arnesen, R. Hallin, and F. Heijkenskjold, *Eur. Phys. J. D* **8**, 227 (2000).
- ²M. C. Castex, *J. Chem. Phys.* **66**, 3854 (1977).
- ³D. E. Freeman, K. Yoshino, and Y. Tanaka, *J. Chem. Phys.* **67**, 3462 (1977).
- ⁴A. Gedanken, J. Jortner, B. Raz, and A. Szöke, *J. Chem. Phys.* **57**, 3456 (1972).
- ⁵O. Cheshnovsky, B. Raz, and J. Jortner, *J. Chem. Phys.* **59**, 3301 (1973).
- ⁶Y. Salamero, A. Birot, H. Brunet, H. Dijols, J. Galy, P. Millet, and J. P. Montagne, *J. Chem. Phys.* **74**, 288 (1981).
- ⁷T. Efthimiopoulos, D. Zouridis, and D. Ulrich, *J. Phys. D* **30**, 1754 (1997).
- ⁸V. Kemper, G. Rieke, F. Veith, and L. Zehnle, *J. Phys. B* **9**, 3081 (1976).
- ⁹D. D. Khadka, Y. Fukuchi, M. Kitajima, K. Hidaka, N. Kouchi, and Y. Hatano, *J. Chem. Phys.* **107**, 2386 (1997).
- ¹⁰F. Spiegelman, F. X. Gadea, and M. C. Castex, *Chem. Phys.* **145**, 173 (1990).
- ¹¹A. P. Hickman, D. L. Huestis, and R. P. Saxon, *J. Chem. Phys.* **96**, 2099 (1991).
- ¹²J. F. Ogilvie and Y. H. Wang, *J. Mol. Struct.* **291**, 313 (1993).
- ¹³S. M. Cybulski and R. R. Toczyłowski, *J. Chem. Phys.* **111**, 10520 (1999).
- ¹⁴I. D. Petsalakis, R. J. Buenker, H.-P. Lieberman, A. Alekseyev, A. Z. Devdariani, and G. Theodorakopoulos, *J. Chem. Phys.* **113**, 5812 (2000).
- ¹⁵I. D. Petsalakis, G. Theodorakopoulos, H.-P. Lieberman, and R. J. Buenker, *J. Chem. Phys.* **115**, 6365 (2001).
- ¹⁶G. Nowak and J. Fricke, *J. Phys. B* **18**, 1355 (1985).
- ¹⁷P. Laporte, P. Gurtler, E. Morikawa, R. Reininger, and V. Saile, *Europhys. Lett.* **9**, 533 (1989).
- ¹⁸T. Tsuchizawa, K. Yamanouchi, and S. Tsuchiya, *J. Chem. Phys.* **92**, 1560 (1990).
- ¹⁹C. D. Pibel, K. Yamanouchi, J. Miyawaki, and S. Tsuchiya, *J. Chem. Phys.* **101**, 10242 (1994).
- ²⁰D. M. Mao, X. K. Hu, S. S. Dimov, and R. H. Lipson, *J. Phys. B* **29**, L89 (1996).
- ²¹G. Gerasimov, R. Khallin, and B. Krylov, *Opt. Spectrosc.* **88**, 176 (2000).
- ²²A. Morozov, B. Krylov, G. Gerasimov, R. Hallin, and A. Arnesen, *Eur. Phys. J. D* **11**, 379 (2000).
- ²³A. Z. Devdariani, A. L. Zagrebin, and K. B. Blagoev, *Ann. Phys. (Paris)* **14**, 467 (1989).
- ²⁴A. L. Zagrebin and N. A. Pavlovskaya, *Opt. Spectrosc.* **69**, 320 (1990).
- ²⁵A. L. Zagrebin and S. I. Tserkovnyi, *Chem. Phys. Lett.* **239**, 136 (1995).
- ²⁶A. B. Alekseyev, H.-P. Lieberman, R. J. Buenker, G. Hirsch, and Y. Li, *J. Chem. Phys.* **100**, 8956 (1994).
- ²⁷A. B. Alekseyev, R. J. Buenker, H.-P. Lieberman, and G. Hirsch, *J. Chem. Phys.* **100**, 2989 (1994).
- ²⁸R. J. Buenker, A. B. Alekseyev, H.-P. Lieberman, R. Lingott, and G. Hirsch, *J. Chem. Phys.* **108**, 3400 (1998).
- ²⁹R. J. Buenker and R. A. Phillips, *J. Mol. Struct.: THEOCHEM* **123**, 291 (1985).
- ³⁰S. Krebs and R. J. Buenker, *J. Chem. Phys.* **103**, 5613 (1995).
- ³¹L. A. LaJohn, P. A. Christiansen, R. B. Ross, T. Atashroo, and W. C. Ermler, *J. Chem. Phys.* **87**, 2812 (1987).
- ³²M. M. Hurley, L. F. Pacios, P. A. Christiansen, R. B. Ross, and W. C. Ermler, *J. Chem. Phys.* **84**, 6840 (1986).
- ³³S. R. Langhoff and E. R. Davidson, *Int. J. Quantum Chem.* **8**, 61 (1974).
- ³⁴L. F. Pacios and P. A. Christiansen, *J. Chem. Phys.* **82**, 2664 (1985).
- ³⁵A. D. McLean and G. S. Chandler, *J. Chem. Phys.* **72**, 5639 (1980).
- ³⁶T. H. Dunning, *J. Chem. Phys.* **55**, 716 (1971).
- ³⁷C. E. Moore, *Atomic Energy Levels As Derived From the Analyses of Optical Spectra, Circular of the National Bureau of Standards* 467, June 1949.
- ³⁸D. Hausamann and H. Morgner, *Mol. Phys.* **54**, 1085 (1985).